Beyond Bloch: A Theoretical Blueprint for Conjugated Polymer Optoelectronics

Miguel Lagos*

Departamento de Física, Facultad de Ciencias, Universidad de Chile, Casilla 653, Santiago, Chile.

Miguel Kiwi[†]

Departamento de Física, Facultad de Ciencias, Universidad de Chile, Casilla 653, Santiago, Chile 7800024, and Centro para el Desarrollo de la Nanociencia y la Nanotecnología, CEDENNA, Avenida Ecuador 3493, Santiago, Chile 9170124.

Rodrigo Paredes[‡]

Facultad de Ingeniería, Universidad Finis Terrae,

Avenida Pedro de Valdivia 1509, Providencia, Santiago, Chile.

(Dated: today)

Conjugated polymers are experiencing a surge of renewed interest due to their promising applications in various organic electronic devices. These include organic light-emitting diodes (OLEDs), field-effect transistors (FETs), and organic photovoltaic (OPV) devices, among many others. Their appeal stems from distinct advantages they hold over traditional inorganic semiconductors. Unlike inorganic semiconductors, where electrons are often considered to be in delocalized, free, or quasifree states (as described by Bloch's theory), electrons in conjugated polymers behave differently. They are strongly coupled within highly localized σ or π -orbitals and interact significantly with the ionic cores. This means they are far from the idealized delocalized states presumed by Bloch's theory approaches. Consequently, after nearly a century of applying Bloch's theory to the electronic transport properties of inorganic materials, there is a clear need for a new theoretical framework to explain efficient charge transport in these organic solids. Our presented model addresses this need by incorporating crucial electron-electron interactions. Specifically, it accounts for both intra-site interactions and interactions between the π -states located at alternating sites along the polymer chain. This framework provides a many-body charge conduction mechanism and explains the semiconducting properties of the undoped material. A significant outcome of our model is the prediction of two novel flat bands of excited bonding states. Intriguingly, these states obey Bose-Einstein statistics and facilitate charge transport. Furthermore, our model accurately reproduces experimental data, providing an excellent fit for measured UV-Vis absorption and electroluminescent spectra.

PACS numbers:

I. INTRODUCTION

Conjugated polymers (CPs) have attracted much attention for a long time, both because of the interesting fundamental physics involved and for their practical applications [1, 2], which even includes materials with promising use in neuromorphic computation [3]. From the theoretical point of view the work by Su, Schrieffer and Heeger [4-6] did set an important milestone. However, the interest on the subject matter was revived recently because of their potential uses. The favorable features of CPs are their easy synthesis and convenient processing, diversity and flexibility. In the CPs the electrons are paired in covalent highly localized σ - or π -orbitals which interact strongly between them and with the ionic cores. One of the aims of this paper is to include, in the theoretical treatment of conjugated polymers, the neighboring sites strong $\pi - \pi$ repulsion, which has proven to be quite significant [7].

In contrast with the importance of their present and potential applications [1], the underlying physics of the semiconducting and conducting properties of conjugated polymers is still at an early stage of understanding. Compared to inorganic semiconductors relatively little is known about the physical origin of the electronic properties of the CPs, and even the precise nature of the semiconductor excitations remains uncertain. Inorganic semiconductors are characterized by the long range single crystal spatial order, where delocalized non-interacting quasi-free electrons in the periodic field of the crystalline lattice provide a reasonable description. In contrast, in organic semiconductors the strict spatial order is often reduced to one dimension, since the different polymeric chains rarely form ordered arrays. More important, the electrons are paired in covalent highly localized σ - or π orbitals which interact strongly among themselves and with the ionic cores, and quasi-free states do not provide a an adequate treatment. Therefore, Bloch's theory for the electronic transport properties of inorganic materials cannot be applied to the CPs, and one has to look for a different theoretical framework for charge transport, since quasi-free Bloch functions are not adequate to char-

*Electronic address: mlagos7@gmail.com †Electronic address: m.kiwi.t@gmail.com ‡Electronic address: raparede@utalca.cl acterize the charge carriers, since the strong repulsion between the π -electrons plays a central role.

CPs are made up by identical molecular chain structures, held together by a sequence of alternate single and double covalent bonds. The double bonds combine a σ - and a π -bond, whereas the single ones are $\sigma - \sigma$ bonds. Hence the backbone is essentially the more stable uniform sequence of σ -bonds. The simplest CP is polyacetylene, for which the periodic molecular structure is just a carbon atom with one of its valence electrons bonded to a hydrogen atom. The metallic state is achieved by doping through local oxidation or reduction. CP thin films attract most of the attention, because of their many present and potential applications in electronic and optoelectronic devices, such as transistors, photodiodes, organic photovoltaic (OPV) devices, organic light-emitting diodes (OLEDs) and many others, in addition to their versatility, and both simple and low fabrication cost. Even the use of paper as a substrate for organic transistors has been a subject of investigation [8].

Some decades ago, devices that combine injected electrons from one electrode and holes from the other one of a two–layer organic emitting diode, were found to have good electroluminescent efficiency under conveniently low operation voltages [9–12]. At present, the use of organic materials as active semiconductors in electronic flat panel displays are in large scale production and commercialization. CPs are intrinsically stable under excitation by an applied voltage or photon capture, both in light emission and harvesting devices. The alternating π –bonds participate actively in the electronic processes leaving intact the primary uniform backbone σ –bonded structure. This backbone provides the necessary stability against degradation by the energy transfer demanded in device operations.

In general, the carbon atoms of the backbone take electrons from neighbouring atoms to form pairs with their four valence electrons in order to create particularly stable octets. Hence the spatial electronic pairing inherent to the π -bonds is taken here as a primary property of conjugate polymers. Charge transport along the polymer chain models must incorporate this fact, and presume that the occurrence of any one-electron elementary process demands an activation energy that is large. Bearing this in mind, we propose an essentially many-body charge transport mechanism which meets the conditions posed by the structure of the conjugated polymers, in a more specific way than the conventional scheme, which was developed for inorganic conductors and semiconductors. Our results are in good agreement with UV-Vis photon absorption experiments [13–18].

II. MODEL

The model put forward here constitutes a generalization of the ideas pioneered by Su, Schrieffer and Heeger [4–6], by adding explicitly the relevant elec-

trostatic repulsion between π -orbitals on neighbouring sites [7]. Chain dimerization is taken for granted and incorporated as an implicit condition. Conduction state charge carriers have only subtle differences with the solitons of Su, Schrieffer and Heeger. Our model Hamiltonian for the polymer chain is

$$H = H_0 + H_{C0} + H_{C1} + H_{T}, \tag{1}$$

where

$$H_0 = \sum_{l} \epsilon \left(n_{l\uparrow} + n_{l\downarrow} \right), \tag{2}$$

with ϵ denoting the energy per electron of the two electrons of the π -orbital and $n_{l\uparrow}=c^{\dagger}_{l\uparrow}c_{l\uparrow},\ n_{l\downarrow}=c^{\dagger}_{l\downarrow}c_{l\downarrow},$ are the two occupation operators of the one–electron states at sites $l=-N/2,-N/2+1,\ldots,N/2$. The $H_{\rm C0}$ term is

$$H_{\rm C0} = \sum_{j} U_0 n_{j\uparrow} n_{j\downarrow},\tag{3}$$

describes the Coulomb repulsion between electrons in π orbitals located on the same site of the polymer chain. Zhang et al. [7] proved that the π - π electrostatic repulsion in conjugated systems has also significant effects in neighbouring sites, while the π - π Pauli repulsion plays a secondary but non-negligible role. The term

$$H_{\rm C1} = \sum_{l} U_1 \left(n_{l+1\uparrow} + n_{l+1\downarrow} \right) \left(n_{l\uparrow} + n_{l\downarrow} \right). \tag{4}$$

accounts for this effect. The two-electron tunneling term

$$H_{\rm T} = \sum_{l} V \left(c_{l+1\uparrow}^{\dagger} c_{l+1\downarrow}^{\dagger} c_{l\downarrow} c_{l\uparrow} + c_{l\uparrow}^{\dagger} c_{l\downarrow}^{\dagger} c_{l+1\downarrow} c_{l+1\uparrow} \right)$$
 (5)

accounts for quantum fluctuations of the π -bonds between neighboring sites. The underlying principle is that the low energy N-electron states of the chain can be expressed as combinations of two-electron π -states localized on every other site along the chain. Hence, any term of the Hamiltonian not having this general structure yields a vanishing contribution when operating on the paired states.

A. Transformation to spin-1/2 operators

In the following sections we will use the just introduced Fermi–Dirac electron representation. However, a transformation to spin 1/2 operators may be also be an advantage. Introducing the new dynamical variables as

$$s_{1}(l) = \frac{1}{2} \left(c_{l\uparrow}^{\dagger} c_{l\downarrow}^{\dagger} + c_{l\downarrow} c_{l\uparrow} \right)$$

$$s_{2}(l) = \frac{1}{2i} \left(c_{l\uparrow}^{\dagger} c_{l\downarrow}^{\dagger} - c_{l\downarrow} c_{l\uparrow} \right)$$

$$s_{3}(l) = \frac{1}{2} \left(n_{l\uparrow} + n_{l\downarrow} - 1 \right) ,$$

$$(6)$$

which satisfy the usual angular momentum commutation relations

$$[s_1, s_2] = is_3$$
 $[s_2, s_3] = is_1$ $[s_3, s_1] = is_2$, (7)

and the Hamiltonian H takes the general form of the Hamiltonian of an anisotropic spin 1/2 antiferromagnetic Heisenberg model

$$H = \sum_{l} \left[\epsilon + 2U_0 + 2U_1 + U_0 s_3(l) \right]$$

$$+ 4U_1 \sum_{l} \left(s_3(l+1)s_3(l) + \frac{V}{2U_1} \left[s_1(l+1)s_1(l) + s_2(l+1)s_2(l) \right] \right).$$
(8)

As the number operators $c_l^{\dagger}c_l$ have eigenvalues 0 and 1, the eigenvalues of s_3 are -1/2, 0 and 1/2. The eigenvalue 0 describes the breaking of a covalent bond, which has a large energy cost. In the limit it becomes infinite the operators s_1 , s_2 , and s_3 behave as the components of a spin 1/2.

In terms of the ladder operators $s_+ = s_1 + is_2$ and $s_- = s_1 - is_2$ H can be rewritten as

$$H = \sum_{l} \left[\epsilon + 2U_0 + 2U_1 + U_0 s_3(l) \right]$$

$$+ 4U_1 \sum_{l} \left(s_3(l+1)s_3(l) + \frac{V}{4U_1} \left[s_+(l+1)s_+(l) + s_-(l+1)s_-(l) \right] \right).$$

$$(9)$$

Since only full occupation is considered, the first sum on the right hand side of Eq. (9) is a constant, and can be ignored. The use of fermion or angular momentum operators are two formally equivalent alternatives to deal with the model put forward here.

III. GROUND STATE AND GROUND STATE ENERGY

A. The ladder operators

Techniques established for handling the anisotropic Heisenberg antiferromagnetic chain can be effectively applied by translating these systems into the fermion scheme. This approach [19-22], starts defining *even* and *odd* operators within the fermion framework.

$$\phi_{e}^{\dagger} = \sqrt{\frac{2}{N}} \sum_{\text{even } l} c_{l+1\uparrow}^{\dagger} c_{l+1\downarrow}^{\dagger} c_{l\downarrow} c_{l\uparrow} + \frac{\alpha}{2} \sqrt{\frac{N}{2}},$$

$$\phi_{o}^{\dagger} = \sqrt{\frac{2}{N}} \sum_{\text{evel } l} c_{l\uparrow}^{\dagger} c_{l\downarrow}^{\dagger} c_{l+1\downarrow} c_{l+1\uparrow} + \frac{\alpha}{2} \sqrt{\frac{N}{2}},$$

$$(10)$$

where $\alpha = V/2U_1$. This sub–section is devoted to derive the main properties of these operators, both the exact ones and their asymptotic limit for strong repulsion between the π -states. Their relevance to the present problem will become apparent in the next subsection.

Recalling the elementary identities between commutators and anticommutators $[A,BC]_-=[A,B]_-C+B[A,C]_-, [AB,C]_-=A[B,C]_-+[A,C]_-B, [A,BC]_-=\{A,B\}_+C-B\{A,C\}_+$ and $[AB,C]_-=A\{B,C\}_+-\{A,C\}_+B,$ where $\{\}_+$ and $[]_-$ correspond to anticommutators and commutators, respectively, and otherwise the usual notation is employed. One can now show the following properties of the ϕ -operators

$$[\phi_{\mathbf{e}}, \phi_{\mathbf{e}}^{\dagger}] = \frac{2}{N} \sum_{\text{even } l} \left[n_{l\uparrow} n_{l\downarrow} \left(1 - n_{l+1\uparrow} - n_{l+1\downarrow} \right) - n_{l+1\uparrow} n_{l+1\downarrow} \left(1 - n_{l\uparrow} - n_{l\downarrow} \right) \right], \tag{11}$$

$$[\phi_{o}, \phi_{o}^{\dagger}] = -\frac{2}{N} \sum_{\text{odd } l} \left[n_{l\uparrow} n_{l\downarrow} \left(1 - n_{l+1\uparrow} - n_{l+1\downarrow} \right) - n_{l+1\uparrow} n_{l+1\downarrow} \left(1 - n_{l\uparrow} - n_{l\downarrow} \right) \right], \tag{12}$$

$$[\phi_{\mathbf{e}}, \, \phi_{\mathbf{o}}] \equiv 0, \tag{13}$$

$$\left[\sum_{l} n_{l\uparrow} n_{l\downarrow}, \phi_{e}^{\dagger}\right] = \sqrt{\frac{2}{N}} \sum_{\text{even } l} c_{l+1\uparrow}^{\dagger} c_{l+1\downarrow}^{\dagger} c_{l\downarrow} c_{l\uparrow} (1 - n_{l\uparrow} - n_{l\downarrow}) + \sqrt{\frac{2}{N}} \sum_{\text{odd } l} c_{l\uparrow}^{\dagger} c_{l\downarrow}^{\dagger} c_{l-1\downarrow} c_{l-1\uparrow} (1 + n_{l\uparrow} + n_{l\downarrow}),$$

$$(14)$$

$$\left[\sum_{l} n_{l\uparrow} n_{l\downarrow}, \phi_{o}^{\dagger}\right] = \sqrt{\frac{2}{N}} \sum_{\text{even } l} c_{l-1\uparrow}^{\dagger} c_{l-1\downarrow}^{\dagger} c_{l\downarrow} c_{l\uparrow} (1 - n_{l\uparrow} - n_{l\downarrow}) + \sqrt{\frac{2}{N}} \sum_{\text{odd } l} c_{l\uparrow}^{\dagger} c_{l\downarrow}^{\dagger} c_{l+1\downarrow} c_{l+1\uparrow} (1 + n_{l\uparrow} + n_{l\downarrow}),$$

$$(15)$$

$$[H_{C1}, \phi_{e}^{\dagger}] = 2U_{1}\sqrt{\frac{2}{N}} \sum_{l \text{ even}} c_{l+1\uparrow}^{\dagger} c_{l+1\downarrow}^{\dagger} c_{l\downarrow} c_{l\uparrow}$$

$$\times (n_{l+2\uparrow} + n_{l+2\downarrow} - n_{l+1\uparrow} - n_{l+1\downarrow} + n_{l\uparrow} + n_{l\downarrow} - n_{l-1\uparrow} - n_{l-1\downarrow} - 2),$$

$$(16)$$

$$[H_{C1}, \phi_{o}^{\dagger}] = 2U_{1}\sqrt{\frac{2}{N}} \sum_{l \text{ odd}} c_{l\uparrow}^{\dagger} c_{l\downarrow}^{\dagger} c_{l+1\downarrow} c_{l+1\uparrow}$$

$$\times (-n_{l+2\uparrow} - n_{l+2\downarrow} + n_{l+1\uparrow} + n_{l+1\downarrow}$$

$$- n_{l\uparrow} - n_{l\downarrow} + n_{l-1\uparrow} + n_{l-1\downarrow} - 2).$$

$$(17)$$

(26)

and

$$H_{\rm T} = \sqrt{\frac{N}{2}} V(\phi_e^{\dagger} + \phi_o^{\dagger} + \phi_e + \phi_o) - N\alpha V.$$
 (18)

In the asymptotic strong conjugation limit

$$n_{l\uparrow} = n_{l\downarrow} \to \begin{cases} 1, & \text{if } l \text{ even} \\ 0, & \text{if } l \text{ odd} \end{cases}$$
 (19)

and the commutators in Eqs. (11) and (12) yield the Bose commutation relations

$$[\phi_{\mathbf{e}}, \, \phi_{\mathbf{e}}^{\dagger}] = [\phi_{\mathbf{o}}, \, \phi_{\mathbf{o}}^{\dagger}] = 1. \tag{20}$$

Also, in the same strong conjugation limit, for long enough polymeric chains one can write

$$[H_{C0}, \phi_{e_0}^{\dagger}] = 0 ,$$
 (21)

and all terms in the two summations on the right-hand sides of Eqs. (14) and (15) cancel in the limit of Eq. (19), except for their first and last terms. A similar argument applies to H_0 , and in the limit of Eq. (19) it also holds, and yields

$$[H_{C1}, \phi_{e,o}^{\dagger}] = 4U_1 \left(\phi_{e,o}^{\dagger} - \frac{\alpha}{2} \sqrt{\frac{N}{2}} \right).$$
 (22)

Therefore, in the strong conjugation limit of Eq. (19) one obtains from Eqs. (1), (18), (20), (21) and Eq. (22) that

$$[H, \phi_{\rm e}^{\dagger}] = 4U_1 \phi_{\rm e}^{\dagger}, \qquad [H, \phi_{\rm o}^{\dagger}] = 4U_1 \phi_{\rm o}^{\dagger}.$$
 (23)

Hence, in the limit of strong conjugation, the operators $\phi_{\rm e}$ and $\phi_{\rm o}$ are ladder operators, which transform any stationary state of H into a state of lower energy. Operators $\phi_{\rm e}^{\dagger}$ and $\phi_{\rm o}^{\dagger}$ have a similar effect, but change the states to higher energy ones. Therefore the ground state $|g\rangle$ of H must satisfy

$$\phi_{\rm e}|g\rangle = \phi_{\rm o}|g\rangle = 0$$
 . (24)

because no stationary state of lower energy can exist.

B. The ground state $|g\rangle$

Defining $|\mathcal{N}\rangle$ as the chain bare of π -electronic states (in the spin representation $|\mathcal{N}\rangle$ is the Néel state)

$$|\mathcal{N}\rangle = \prod_{\text{even }l} c_{l\uparrow}^{\dagger} c_{l\downarrow}^{\dagger} |0\rangle,$$
 (25)

where $|0\rangle$ is the vacuum, that is the naked backbone of σ -bonds, and introducing the operator Λ as

$$\begin{split} & \Lambda = \sqrt{\frac{N}{2}} \left(\phi_{\rm e}^{\dagger} + \phi_{\rm o}^{\dagger} - \phi_{\rm e} - \phi_{\rm o} \right) \\ & = \sum_{l} (-1)^{l} \left(c_{l+1\uparrow}^{\dagger} c_{l+1\downarrow}^{\dagger} c_{l\downarrow} c_{l\uparrow} - c_{l\uparrow}^{\dagger} c_{l\downarrow}^{\dagger} c_{l+1\downarrow} c_{l+1\uparrow} \right) \,, \end{split}$$

it is shown next that in the asymptotic limit of Eq. (19) the ground state of H is given by

$$|g\rangle = \exp\left(-\frac{\alpha}{2}\Lambda\right)|\mathcal{N}\rangle.$$
 (27)

To demonstrate the validity of Eq. (27) notice that it can be proven by complete induction that, in the strong conjugation limit of Eq. (19), it yields

$$[\phi_{e,o}, (\phi_e^{\dagger} + \phi_o^{\dagger} - \phi_e - \phi_o)^n] = n(\phi_e^{\dagger} + \phi_o^{\dagger} - \phi_e - \phi_o)^{n-1}$$
(28)

for $n = 0, 1, 2, \ldots$, hence for any analytic function F with derivative F'

$$[\phi_{\mathrm{e,o}}, F(\phi_{\mathrm{e}}^{\dagger} + \phi_{\mathrm{o}}^{\dagger} - \phi_{\mathrm{e}} - \phi_{\mathrm{o}})] = F'(\phi_{\mathrm{e}}^{\dagger} + \phi_{\mathrm{o}}^{\dagger} - \phi_{\mathrm{e}} - \phi_{\mathrm{o}}). \tag{29}$$

Applying this property with F substituted by the exponential function appearing in Eq. (27) and the definitions of Eq. (10), it can readily be shown that $|g\rangle$ satisfies Eqs. (24) and is therefore the ground state in the strong conjugation limit Eq. (19). Notice that the ground state Eq. (27) is not perturbative because of the large factor $\sqrt{N/2}$ multiplying the sum Eq. (26) that defines Λ .

C. The ground state energy E_g

To determine the ground state energy the commutation property of Λ

$$[c_{l\uparrow}^{\dagger}c_{l\downarrow}^{\dagger}, \Lambda] = (-1)^{l} \left(c_{l+1\uparrow}^{\dagger}c_{l+1\downarrow}^{\dagger} + c_{l-1\uparrow}^{\dagger}c_{l-1\downarrow}^{\dagger}\right) \left(n_{l\uparrow} + n_{l\downarrow} - 1\right),$$
(30)

is required, which in the asymptotic limit Eq. (19), after iterating ν times, it reads

$$[[\dots [c_{l\uparrow}^{\dagger}c_{l\downarrow}^{\dagger}, \Lambda], \Lambda], \dots, \Lambda]_{\nu \text{ times}}$$

$$= (-1)^{l\nu} (-1)^{\nu(\nu+1)/2} (\tau + \tau^{-1})^{\nu} c_{l\uparrow}^{\dagger} c_{l\downarrow}^{\dagger},$$
(31)

where τ is the nearest neighbor translation operator

$$\tau c_{ls} = c_{l+1s} \quad \tau^{-1} c_{ls} = c_{l-1s} \quad s = \uparrow, \downarrow. \tag{32}$$

Combining this with the identity

$$e^{-B}A e^{B} \equiv A + \frac{1}{1!}[A, B] + \frac{1}{2!}[[A, B], B] + \frac{1}{3!}[[[A, B], B], B] + \cdots,$$
(33)

the generating function of the modified Bessel functions $I_{\nu}(z)$

$$\exp\left[\frac{z}{2}(\tau+\tau^{-1})\right] = \sum_{\nu=-\infty}^{\infty} I_{\nu}(z)\tau^{\nu}, \tag{34}$$

and the property $J_{\nu}(z) = i^{-\nu}I_{\nu}(iz)$, where J_{ν} is the unmodified Bessel function, it can be shown that

$$\exp\left(\frac{\alpha}{2}\Lambda\right)c_{l\uparrow}^{\dagger}c_{l\downarrow}^{\dagger}\exp\left(-\frac{\alpha}{2}\Lambda\right)$$

$$=\sum_{\nu=-\infty}^{\infty}(-1)^{l\nu}(-1)^{\nu(\nu+1)/2}J_{\nu}(\alpha)c_{l+\nu\uparrow}^{\dagger}c_{l+\nu\downarrow}^{\dagger}.$$
(35)

Eq. (35) in combination with Eq. (27) are now used to calculate expectation values. In particular, the average occupation of a site l is

$$\langle g|(n_{l\uparrow} + n_{l\downarrow})|g\rangle = 1 + (-1)^l J_0(2\alpha) , \qquad (36)$$

where J_{ν} is the usual Bessel function of order ν . The short range correlation coefficient is

$$\frac{1}{N}\langle g|\sum_{l} \left(n_{l+1\uparrow}+n_{l+1\downarrow}\right) \left(n_{l\uparrow}+n_{l\downarrow}\right) |g\rangle = 1 - [J_0(2\alpha)]^2.$$

The energy of the ground state $E_g = \langle g | (H_0 + H_{C1} + H_T) | g \rangle$ is given by

$$E_g = N\epsilon + NU_1 [1 - (J_0(2\alpha))^2 + 2\alpha J_1(2\alpha)]$$
 (38)

In obtaining Eqs. (36), (37) and Eq. (38) use was made of Neumann's addition formulas of the Bessel functions and Graf's generalization of them [23]. The previous results expressed in terms of the Bessel functions look elegant, but it must be kept in mind that they hold only in the asymptotic limit Eq. (19), that is when α is sufficiently small. Up to second order in α one has that

$$E_{a} = 4NU_{1}(\alpha^{2} + 0(\alpha^{4})) . {39}$$

Using the properties of the ladder operators $\phi_{\rm e}^{\dagger}$ and $\phi_{\rm o}^{\dagger}$, given by Eq. (23), yields the set of eigenvectors

$$|n_{\rm e} n_{\rm o}\rangle = \frac{(\phi_{\rm e}^{\dagger})^{n_{\rm e}}}{\sqrt{n_{\rm e}!}} \frac{(\phi_{\rm o}^{\dagger})^{n_{\rm o}}}{\sqrt{n_{\rm o}!}} |g\rangle, \quad n_{\rm e}, n_{\rm o} = 0, 1, 2, 3, \dots$$
(40)

which are eigenvectors of H, with eigenenergies

$$E_{n_{\rm e}n_{\rm o}} = 4(n_{\rm e} + n_{\rm o})U_1 + E_q.$$
 (41)

The theoretical framework described up to this point would not be complete without including the fact that the ground state is twofold degenerate. In effect,

$$|\bar{g}\rangle = \exp\left(\frac{\alpha}{2}\Lambda\right) |\bar{\mathcal{N}}\rangle, \quad |\bar{\mathcal{N}}\rangle = \prod_{\text{odd }l} c_{l\uparrow}^{\dagger} c_{l\downarrow}^{\dagger} |0\rangle, \quad (42)$$

is also an eigenvector of H with the same energy eigenvalue Eq. (38). The bosonic operators $\phi_{\rm e}$ and $\phi_{\rm o}$ become creation operators when operating on $|\bar{g}\rangle$.

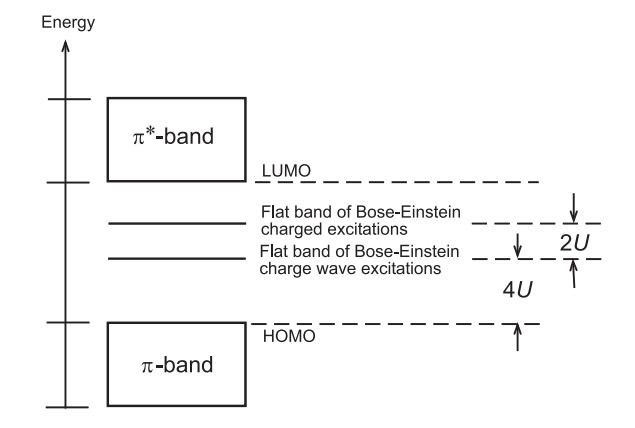


FIG. 1: The π - π repulsion gives rise to two Bose–Einstein excitations energy levels, whose energies lie inside the gap 4U and 6U above the energy of the highest occupied molecular orbital (HOMO).

Fig. 1 shows a schematic diagram of the energy spectrum of the molecular chain. The π - π repulsion yields a novel energy level of Bose-Einstein excitations located between the HOMO and LUMO energies. Hence, the conduction band in this framework is not made up by electrons in extended anti-bonding states, but by electronic pairs excited to the novel flat band of energy 4U. Certainly the system has other degrees of freedom, additional to the ones described by the operators ϕ_e and $\phi_{\rm o}$, e.g. the solitons first invoked by Su, Schrieffer and Heeger [4, 5] for polyacetilene, and later generalized to other conjugate polymers [6]. They give rise to the flat band of energy $6U_1$ in Fig. 1, which we will address in detail, after we show how the excitations associated with the operators ϕ_e and ϕ_o transport momentum and energy. As it is assumed that one-electron processes involve large activation energies, the momentum operator \vec{P} must be written as the two-particle operator

$$\vec{P} = -\frac{i\hbar}{2} \int d^3r' \ d^3r \ \Psi^{\dagger}(\vec{r'}, t) \Psi^{\dagger}(\vec{r}, t)$$

$$\times (\nabla' + \nabla) \Psi(\vec{r}, t) \Psi(\vec{r'}, t) + \text{ adjoint operator,}$$
(43)

and in terms of the electron field operator it reads

$$\Psi(\vec{r},t) = \sum_{ls} c_{ls} w_s(\vec{r} - la\hat{\imath}). \tag{44}$$

Here ∇' and ∇ are the gradient operators with respect to $\vec{r'}$ and \vec{r} , and $w_s(\vec{r} - la\hat{\imath})$ represents the one–particle wave function of an electron in a covalent π state at site l, a is the distance between nearest neighbor sites of the polymer chain, and $\hat{\imath}$ is the unitary vector along the chain direction. Because of analytical reasons, and the small overlap of functions w_s centered on neighboring sites

$$\int d^3r \, w_s^*(\vec{r} - l'a\hat{\imath}) \nabla w_s(\vec{r} - la\hat{\imath}) = \begin{cases} 0, & \text{if } l = l' \\ q \, \hat{\imath} & \text{if } l' = l+1 \\ -q^* \, \hat{\imath} & \text{if } l' = l-1 \\ 0, & \text{otherwise} \end{cases}$$
(45)

Inserting Eqs. (44) and (45) into Eq. (43), the resulting expression for \vec{P} finally reduces to the same standard equation for the one–particle momentum operator. However, one must recall that the polymer backbone is not rigid, and the alternating occupied and unoccupied π -orbitals cause a dimerization of the polymer chain. Hence, the occupied and virtual π -orbitals are expected to have finite energy differences, simply because of the broken periodicity of the distance between the positive charges involved in the chemical bonds. In Eq. (45) the parameter a takes slightly different values if the accompanying index l is even or odd. When taking this into consideration the momentum operator splits into a one–particle and a two–particle term, and takes the general form

$$\vec{P} = -i\hbar \, q \, \hat{i} \sum_{l,s} \left(c_{l+1,s}^{\dagger} c_{ls} - c_{l,s}^{\dagger} c_{l+1,s} \right)
- i\hbar \, \gamma q \, \hat{i} \sum_{l} \left(c_{l+1\uparrow}^{\dagger} c_{l+1\downarrow}^{\dagger} c_{l\downarrow} c_{l\uparrow} - c_{l\uparrow}^{\dagger} c_{l\downarrow}^{\dagger} c_{l+1\downarrow} c_{l+1\uparrow} \right),$$
(46)

where γ is a coefficient proportional to the shift δa of the bond lengths of the dimerized chain. In general, the first term of \vec{P} in Eq. (46) destroys pairs and the second one always conserves them. As H and the eigenstates Eq. (27), Eq. (40) and Eq. (42) involve just paired electrons, consistent with the principle that one–electron processes involve too large activation energies, it is sufficient to retain just the second term and write \vec{P} as

$$\vec{P} = -i\hbar \gamma q \,\hat{\imath} \sqrt{\frac{N}{2}} \left(\phi_{\rm e}^{\dagger} - \phi_{\rm o}^{\dagger} - \phi_{\rm e} + \phi_{\rm o} \right) \,. \tag{47}$$

In the Heisenberg picture

$$\frac{d^2P}{dt^2} = -\frac{1}{\hbar^2}[H, [H, P]] \tag{48}$$

and using Eqs. (47) and (23) one has that

$$\frac{d^2P}{dt^2} = -\frac{4U_1^2}{\hbar^2}P \ . \tag{49}$$

Eq. (49) shows that the operators $\phi_{\rm e}^{\dagger}$ and $\phi_{\rm o}^{\dagger}$ excite collective charge motion modes of the chain π -bonds. The collective oscillation involves charge displacements of the angular frequency $\omega = 2U_1/\hbar$, independent of the polymer chain length. Hence, resonances favouring charge transfer with neighbouring chains are expected to occur.

The model worked out above shows that the dynamical effect of the π - π repulsion in conjugate polymers is a set of degenerate excited states, which can transport charge along the polymer chain. These novel states obey Bose–Einstein statistics and have energy eigenvalues that form a flat band located $4U_1$ above the ground state, in the HOMO-LUMO gap. The model assumed in this step provides a natural answer to the question of how the repulsion between the π -orbitals affects the dynamics of the system, however it still is a bit too simple. An important conclusion is that the single frequency $\omega = 2U_1/\hbar$, common to all the polymeric chains in the sample, no matter their length, are expected to produce resonances that enhance the probability of charge transfer.

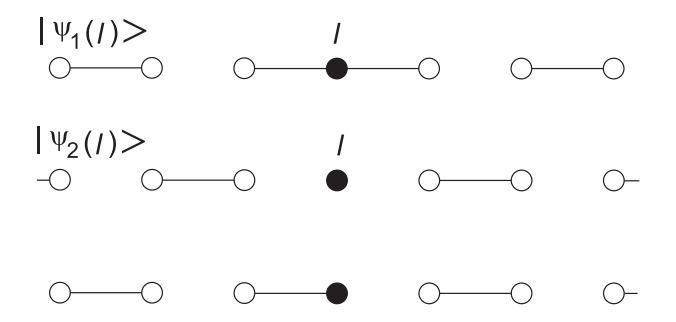


FIG. 2: Circles represent monomers and lines the π -bonds. The filled black circles are for reference only. The upper and middle illustrations represent the hybrid states $|\psi_1\rangle$ and $|\psi_2\rangle$, respectively. The bottom configuration represents one of the two degenerate ground states.

D. Metallic phase

The metallic phase is made up by a superposition of excited states, quite similar to those introduced by Su et al. [4–6]. At any site l the π -orbital occupation changes from even to odd, or vice-versa. The monomer in between marks a boundary between the two degenerate ground states, $|g\rangle$ and $|\bar{g}\rangle$, that prevail at either side of the monomer. The energy of this state can be inferred from a heuristic argument. First consider a class of excited states of the form $(|\psi_1(l)\rangle \pm |\psi_2(l)\rangle)/\sqrt{2}$, where $|\psi_1(l)\rangle$ and $|\psi_2(l)\rangle$ are the states represented schematically in Fig. 2. As the interaction between the orbitals is limited to nearest neighbors, for α small enough the mutual perturbation of the states at the two sides of l is small.

Therefore, the combined energy contribution from both sides totals approximately $4U_1$. Additionally, the energy contribution from the central parts at site l of $|\psi_1(l)\rangle$ and $|\psi_2(l)\rangle$ can be estimated in zeroth order in α as 4U and 0, respectively. Hence, the contribution to the energy of the central part is the average value 2U between these two figures, which added to the energy 4U of the two sides gives an estimate of $6U_1$ for the total energy of the combined states $(|\psi_1(l)\rangle \pm |\psi_2(l)\rangle)/\sqrt{2}$. This class of excited states configures the upper flat band of charged excitations illustrated in Fig. 1. The excitations have a charge of $\pm 2e$ and an energy $6U_1$ above the energy of the highest occupied molecular orbital (HOMO). We understand that the energy of the HOMO incorporates the energy Eq. (38) for the vacuum of the new excitations. The metallic phase is given by the linear combination

$$|k\rangle = \sqrt{\frac{1}{N}} \sum_{l=-N/2}^{N/2} \exp(ikl) |\psi_p(l)\rangle , \quad k = \frac{2\pi}{N} n,$$

$$p = 1, 2 \qquad n = -\frac{N}{2}, \dots, -1, 0, 1, 2, \dots, \frac{N}{2}.$$
(50)

We now compute the experimentally measurable results that the above model yields.

IV. COMPARISON WITH EXPERIMENT

The predictions obtained with the above model for the energy bands can readily be tested by light absorption spectra. The two prominent flat bands observed in Fig. 1 are particularly characteristic, notably exhibiting an approximate energy ratio of 3/2. This distinctive feature was examined by Chen et al. [13] through their measurements of the electromagnetic radiation absorption spectra of a 60-nm thick film of the conjugated polymer FBT-Th₄(1,4) in the 300–800 nm wavelength interval. The target polymer was a solid film; however, solutions in chlorobenzene and dichlorobenzene gave very similar results. Two main maxima, at $\lambda_1 = 692$ nm and $\lambda_2 = 453$ nm were observed; their energies are $\epsilon_1 = 1.792 \text{eV}$ and $\epsilon_2 = 2.737 \text{eV}$, and their ratio is

$$\frac{\epsilon_2}{\epsilon_1} = 1.527,\tag{51}$$

which is very close to the estimated 3/2 value. The accuracy of the agreement is quite unexpected, because the spectral maxima are displaced from the actual transition energy by Stokes shifts; however, the two maxima displacements are expected to be quite similar, which may explain such a good agreement. The rest of the experimental spectrum also is in good agreement with the energy level scheme of Fig. 1; in fact, the maximum between a plateau and a zero absorption region are evidence of an energy gap.

More recent observations of the UV-Vis excitation spectra, of many conjugated polymers of interest, show

results similar to those of Chen et al. [13], with the ratio of Eq. (51) ranging between 1.4 and 1.7 [14–18]. The spectra shows two main peaks, centered typically at $\lambda_1 \approx 700\,\mathrm{nm}$ and $\lambda_2 \approx 450\,\mathrm{nm}$, with a full width at half maximum of about 100 nm, as illustrated in Fig. 3.

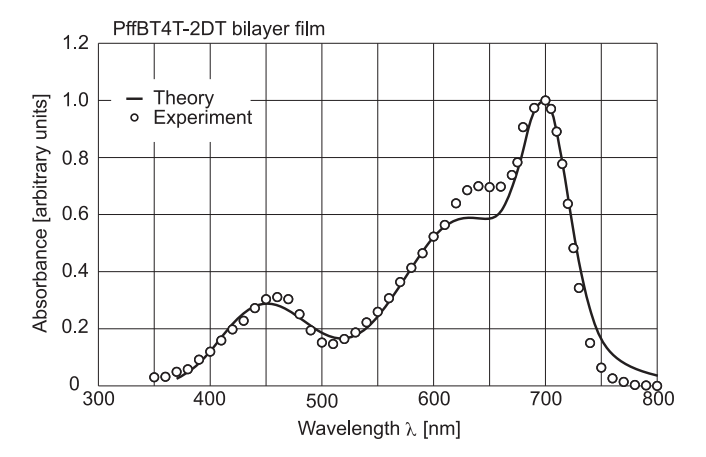


FIG. 3: Open circles illustrate experimental results for the UV–Vis bsorption spectra of a thin film of the organic semi-conductor PffBT4T-2DT, a conjugate polymer [15]. The full line is a rough theoretical estimate of the processes, assuming the excitation of three sharp energy levels, that correspond (from left to right) to wavelengths 620, 830 and 752 nm for the three wide peaks. The large widths and shifts of the maxima are due to the multiphonon character of the processes. Just bulk substrate modes were considered in the estimate, which shows that the observed absorption bands can be explained on the basis of a few sharp energy levels.

However, the most remarkable feature of the measured spectra is that the absorption and emission bands can be explained by the excitation and de-excitation of a few states of sharply defined energies, as those predicted in the previous sections. A typical example is given in Fig. 3, where the open circles represent the photon absorbance of a thin layer of the semiconductor CP PffBT4T-2DT, measured by Li et al. [15]. The solid line is a theoretical estimate, which assumes that photon absorption takes place by the excitation of three sharp levels of energies 2.00, 1.49 and 1.65 eV (wavelengths 620, 830 and 752 nm, respectively). The three absorption lines are significantly widened and shifted by multiphonon events that accompany the excitation process. The excitation of a bonding orbital necessarily involves a sudden distortion of the molecular environment, which excites the vibration modes, particularly the acoustic ones. Since the entropy increases the vibration modes exchange energy at random, but with an average energy gain. This widens the spectral peaks and shifts them to shorter wavelengths (Stokes shift) as they absorb photons. The 620 nm level becomes a wide line that peaks around 450 nm, while the 830 nm level contributes the largest intensity, and is significantly broadened giving rise to the shoulder at ~ 650 nm. Finally, the 752 nm state is only slightly broadened and manifests itself as the narrow peak at

700 nm.

The fit of the theoretical curve of Fig. 3, was obtained following the procedure described in detail by Lagos and Paredes [24]. It should be mentioned that it is obtained using some rather crude hypotheses. However, the results clearly exhibit what is most relevant: that the observed spectral features can be explained by the excitation of three sharply defined energy levels. The theoretical curve of Fig. 3 assumes that the absorbing orbital is in a tetrahedral symmetry environment, and that the vibrational modes are the bulk substrate modes. More accurate results would demand a more detailed study, in particular the incorporation of surface modes, but the present estimate is sufficient for the purposes of what we intend to convey. Our point is that the absorption curves can be explained by a finite number of sharp energy levels, as opposed to a finite width energy band. Moreover, the absorption spectra of the semiconducting CPs are quite similar. The largest wavelength peak always has a shoulder, and in general the spectra exhibit two main peaks clearly attributable to the two flat bands, as derived above. To obtain precise values for the discrete energy levels above the HOMO energy from the UV-Vis excitation spectra demands the deconvolution of the vibrational modes which widen the spectral lines [24].

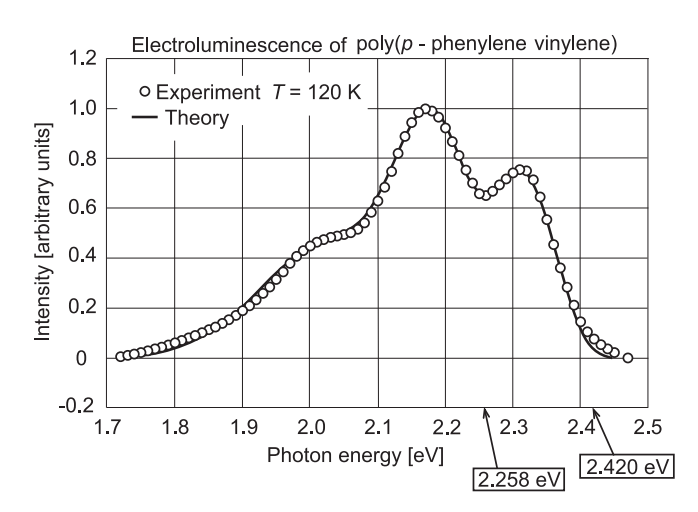


FIG. 4: Electroluminescent emission by an organic diode made of the conjugate polymer poly(p-phenylene vinylene). Circles represent the classical experimental work of Burroughes et al. [11] and the solid line a calculation considering the emission by two electronic energy levels of 2.258 and 2.420 eV. The peaks are shifted, widened and split by multi-phonon events.

Fig. 4 shows the emission spectrum of an electroluminiscent device made of the CP poly(p–phenylene vinylene), published in a seminal paper of Burroughes et al. [11]. Open circles describe the experimental results at a temperature $T=120\,\mathrm{K}$, and the solid line is the emission spectrum calculated with the same procedure described by Lagos and Paredes [24], in relation to Fig. 3. Phonon widening and shift of the spectral maxima are

particularly strong. The spectrum shows three peaks, but the calculation assumes only two electronic energy levels, corresponding to 2.258 and 2.420 eV, shown in Fig. 4 with an arrow pointing to their positions along the energy axis. The large Stokes shifts caused by the vibration modes are quite evident, and is the cause of the split of the spectral feature split into two maxima.

V. SUMMARY AND CONCLUSIONS

We developed a model for covalent conjugate polymers including the interaction between π -bonds. It is based on two hypothesis: i) that the covalent character of the π -bonds, forming stable octets, is relevant in transport processes. This may be seen as a sort of pairing in coordinate space. ii) The explicit introduction of the repulsion between the π -bonds of nearest neighbor sites.

The localized character of the two–particle states is not inconsistent with their capability for transporting momentum, energy and charge. We formulate a many–body model leading to transport under these conditions. A few very narrow energy bands with no dispersion are predicted in the gap between the energies of the HOMO and the LUMO. The novel bands are able to host many electron pairs that obey Bose–Einstein statistics. The potential for charge transport is very large. In fact, charge transport in inorganic conductors is due to electrons in a narrow fringe around the Fermi energy, and it turns out that in this model the overwhelming majority of the π –orbitals does participate in the conduction.

Due to the localized nature of bonding in nonconjugated polymers, the interactions between a monomer's constituent parts lead to a discrete and well-These sharp endefined spectrum of energy levels. ergy levels become finite width energy bands when the monomers bond together to form a polymer of considerable length. Therefore, in principle, the observation of spectral lines of well defined energy, that originate in sharp energy levels of the spectra of non-conjugated polymers, are not expected. Traditionally, luminescence from polymeric luminogens is attributed to the presence of conjugated structures [25]. In this paper it is shown that the bands of conjugated polymers are due to transitions between discrete energy levels of sharply defined energy. The line width and shape observed in the optical spectra are determined by the strong coupling with the vibrational modes, particularly the acoustic ones. These discrete energy levels are due to π -orbital repulsion. The competition of the next nearest neighbouring π -orbitals that try to occupy the intermediate almost empty site, and the strong repulsion between them, generates an effect similar to the energy and momentum transmission in a hard elastic ball line [26]. Therefore, charge conduction and the observation of absorption and emission spectral features are evidence for the existence of a few sharp energy levels, in the energy gap above the HOMO energy, and are closely related features of conjugated polymers.

Acknowledgements MK was partially supported by Financiamiento Basal para Centro Investigación Avanzada

ANID, grant CIA25002.

- [1] T.-H. Le, Y. Kim, H. Yoon, Polymers 2017, 9, 150.
- [2] M. P. Estarellas, I. D'Amico, Timothy P. Spiller, Sci. Repts. 2017, 7, 42904.
- [3] Shuzhi Liu, Jianmin Zeng, Zhixin Wu, Han Hu, Ao Xu, Xiaohe Huang, Weilin Chen, Qilai Chen, Zhe Yu, Yinyu Zhao, Rong Wang, Tingting Han, Chao Li, Pingqi Gao, Hyunwoo Kim, Seung Jae Baik, Ruoyu Zhang, Zhang Zhang, Peng Zhou, Gang Liu, Nature Comm. 2023, 14, 7655.
- [4] W. P. Su, J. R. Schrieffer, A. J. Heeger, Phys. Rev. Lett. 1979, 42, 1698.
- [5] W. P. Su, J. R. Schrieffer, A. J. Heeger, *Phys. Rev. B* 1980, 22, 2099.
- [6] A. J. Heeger, S. Kivelson, J. R. Schrieffer, W. P. Su, Rev. Mod. Phys. 1988, 60, 781.
- [7] H. Zhang, X. Jiang, W. Wua, Y. Mo, Phys. Chem. Chem. Phys. 2016, 18 11821.
- [8] U. Zschieschang, H. Klauk, J. Mater. Chem. C 2019, 7, 5522.
- [9] C. W. Tang, S. A. Vanslyke, Appl. Phys. Lett. 1987, 51, 913
- [10] C. Adachi, T. Tsutsui, S. Saito, Appl. Phys. Lett. 1989, 55, 1489.
- [11] H. Burroughes, D. D. C. Bradley, A. R. Brown, R. N. Marks, K. Mackay, R. H. Friend, P. L. Burns, A. B. Holmes, *Nature* 1990, 347, 539.
- [12] D. Braun, A. J. Heeger, Appl. Phys. Lett. 1991, 58, 1982.
- [13] Z. Chen, P. Cai, J. Chen, X. Liu, L. Zhang, L. Lan, J. Peng, Y. Ma, Y. Cao, Adv. Mat. 2014, 26, 2586.

- [14] Y. Yao, H. Dong, F. Liu, T. P. Russell, W. Hu, Adv. Mat. 2017, 29, 1701251.
- [15] M. Li, D. K. Mangalore, J. Zhao, J. H. Carpenter, H. Yan, H. Ade, H. Yan, K. Müllen, P. W. M. Blom, W. Pisula, D. M. de Leeuw, K. Asadi, *Nature Commun.* 2018, 9, 451.
- [16] X. Li, X. Liu, P. Sun, Y. Feng, H. Shan, X. Wu, J. Xu, C. Huang, Z–K. Chen, Z–X. Xu, RSC Adv. 2017, 7, 17076.
- [17] J. H. Lee, C. G. Park, A. Klm, H. J. Kim, Y. Kim, S. Park, M. J. Cho, D. H. Choi, ACS Applied Materials & Interfaces 2018, 10, 22, 18974.
- [18] K. S. Park, J. J. Kwo, R. Dilmurat, G. Qu, P. Kafle1, X. Luo, S-H. Jung, Y. Olivier, J-K. Lee, J. Mei, D. Beljonne, Y. Diao, Sci. Adv. 2019, 5, eaaw7757.
- [19] M. Lagos, G. G. Cabrera, Phys. Rev. B 1988, 38, 659.
- [20] M. Lagos, M. Kiwi, E. R. Gagliano, G. G. Cabrera, Sol. State Commun. 1988, 67, 225.
- [21] G. G. Cabrera, M. Lagos, M. Kiwi, Sol. State Commun. 1988, 68, 743.
- [22] D. Gottlieb, M. Lagos, M. Montenegro, Sol. State Commun. 1992 81, 729.
- [23] G. E. N. Watson, A Treatise on the Theory of the Bessel Functions, 2nd edition, p. 359, Cambridge, London, 1966.
- [24] M. Lagos, R. Paredes, J. Phys. Chem. A 2014, 118,
- [25] W-F. Lai, Journal of Drug Delivery Science and Technology 2020 59, 101916.
- [26] C. Lehmann, M. Rosenbauer, Am. J. Phys. 1980 48, 496.